Reformulation of thermally assisted-occupation density functional theory in the Kohn-Sham framework

Cite as: J. Chem. Phys. 156, 174108 (2022); doi: 10.1063/5.0087012 Submitted: 31 January 2022 • Accepted: 14 April 2022 • Published Online: 3 May 2022







Shu-Hao Yeh, 1,2,3 Weitao Yang, 3,4) and Chao-Ping Hsu 1,3,4,b)





AFFILIATIONS

- ¹Institute of Chemistry, Academia Sinica, Taipei 11529, Taiwan
- ²Department of Chemistry, National Taiwan University, Taipei 10617, Taiwan
- ³Department of Chemistry, Duke University, Durham, North Carolina 27710, USA
- ⁴National Center for Theoretical Sciences, Taipei 10617, Taiwan
- ^{a)}E-mail: weitao.yang@duke.edu
- b) Author to whom correspondence should be addressed: cherri@sinica.edu.tw

ABSTRACT

We reformulate the thermally assisted-occupation density functional theory (TAO-DFT) into the Kohn-Sham single-determinant framework and construct two new post-self-consistent field (post-SCF) static correlation correction schemes, named rTAO and rTAO-1. In contrast to the original TAO-DFT with the density in an ensemble form, in which each orbital density is weighted with a fractional occupation number, the ground-state density is given by a single-determinant wavefunction, a regular Kohn-Sham (KS) density, and total ground state energy is expressed in the normal KS form with a static correlation energy formulated in terms of the KS orbitals. In post-SCF calculations with rTAO functionals, an efficient energy scanning to quantitatively determine θ is also proposed. The rTAOs provide a promising method to simulate systems with strong static correlation as original TAO, but simpler and more efficient. We show that both rTAO and rTAO-1 is capable of reproducing most results from TAO-DFT without the additional functional E_{θ} used in TAO-DFT. Furthermore, our numerical results support that, without the functional E_{θ} , both rTAO and rTAO-1 can capture correct static correlation profiles in various systems.

Published under an exclusive license by AIP Publishing. https://doi.org/10.1063/5.0087012

I. INTRODUCTION

The electronic structure computation has been a powerful tool for quantitative prediction of physical and chemical properties of isolated molecules and extended systems, which transformed the modern research paradigm as it boosts the exploration and prediction of both known and uncharted systems and reactions. Among the vast selection of methodologies, the density functional theory (DFT)¹⁻³ plays a dominant role in many applications due to its relatively good performance and mild computational complexity. 4-6

Despite a formally exact theory, DFT with currently developed approximate exchange-correlation (XC) functionals is still prone to many problems.⁶⁻⁹ Among them, problems for systems with nearly degenerate frontier orbitals, a common feature in bond-dissociation and transition state of a chemical reaction, have been well-characterized, which is very similar to

the static or nondynamical correlation problem for wavefunction theories. 10 While the dynamic correlation for wavefunction theories is provided by post-self-consistent-field (SCF) treatments, such as configuration interaction (CI) methods and coupled-cluster (CC) methods, multi-reference approaches, complete-active-space (CAS) SCF, ^{11,12} restricted-active-space (RAS) SCF, ^{13,14} are useful schemes for static correlations, where energetically similar orbitals and their corresponding configurations are treated equivalently. For DFT, the correlation component of XC potential is often regarded as an inclusion of the dynamical correlation. The problems of nearly degenerate frontier orbitals still exist in most DFT with common XC functionals, and generalizations of multi-reference method for DFT have been suggested. 15-19 However, in those methods, problems remain in the choice of active space and convergence, such as the strong dependence of initial guess, and the steep increase of computational complexity to the size of active space.²⁰ Alternatively, modeling static correlation through XC-functional has been developed and implemented. ^{10,21–25}

Treatment of static correlation with a mild computational complexity has been an important direction of modern computational quantum chemistry. The necessary condition for correctly treating static correlation in DFT has been established with the exact degeneracy requirement in terms of fractional spins. ^{26–28} Novel approaches, including fractional-spin localized orbital scaling correction (FSLOSC),²⁵ have been developed. On the other hand, schemes based on linear response theory, such as spin–flip time-dependent DFT (SF-TDDFT)^{29–32} and particle–particle random phase approximation, ^{18,33} are useful solutions for some, but not general problems with static correlation. The thermally assisted-occupation density functional theory (TAO-DFT) is an interesting approach for static correlation with much potential, ^{34,35} which is the basis of the present work.

Instead of the density of a single determinant in the Kohn–Sham density functional theory (KS-DFT), in TAO-DFT, ^{34,35} the electron density is expressed as

$$\rho_f(\mathbf{r}) = \sum_p f_p \, \phi_p^*(\mathbf{r}) \phi_p(\mathbf{r}), \tag{1}$$

where the orbital electron density $\phi_p^* \phi_p$ is weighted by a Fermi–Dirac function of orbital ε_p energy,

$$f_p = \left[1 + \exp\left(\frac{\varepsilon_p - \mu}{\theta}\right)\right]^{-1}.$$
 (2)

Here, μ and θ are the chemical potential and the fictitious temperature, respectively. We note that θ can be viewed as a measure for the strength of static correlation, which is a system-dependent parameter, while μ is determined by keeping the total particle number a constant. With this modification on the density expression, the total energy functional was recast accordingly as

$$E^{\text{TAO}} = T_s^{\theta} [\{ \varepsilon_p, \phi_p \}] + E_{\text{ext}}[\rho_f] + E_{\text{H}}[\rho_f] + E_{\text{xc}}^{\text{DFA}}[\rho_f] + E_{\theta}[\rho_f]$$

$$+ \theta \sum_{p} [f_p \ln f_p + (1 - f_p) \ln(1 - f_p)],$$
(3)

where the terms on the right-hand side are noninteracting kinetic energy, external potential energy, Hartree (classical Coulomb), exchange–correlation (XC) energy evaluated from a density-functional approximation (DFA), and θ energy and entropic energy term. E_{θ} is defined and evaluated approximately as the difference between the noninteracting free energy at zero temperature and that at temperature θ , ³⁴

$$E_{\theta} = T_{s}[\rho] - A_{s}^{\theta}[\rho]. \tag{4}$$

We note that

$$A_s^{\theta}[\rho] = T_s^{\theta}[\{\varepsilon_p, \phi_p\}] + \theta \sum_p [f_p \ln f_p + (1 - f_p) \ln(1 - f_p)]$$
 (5)

and $A_s^{\theta=0}[\rho] = T_s[\rho]$. In numerical calculation for E_θ , Eqs. (4) and (5) were not used, instead a local density approximation was used for both $T_s[\rho]$ and $A_s^{\theta}[\rho]$.³⁴ We note that even though many terminologies in TAO-DFT are borrowed from statistical mechanics and thermodynamics, TAO-DFT is still an ground-state electronic

theory for a pure state. Similar to conventional DFT, a variational principle with respect to orbitals can be applied on the total energy, and the resulting eigenvalue equation is

$$\left[-\frac{1}{2} \nabla_{\mathbf{r}}^{2} + v_{\text{ext}}(\mathbf{r}) + v_{\text{H}}[\rho_{f}](\mathbf{r}) + v_{\text{xc}}^{\text{DFA}}[\rho_{f}](\mathbf{r}) + v_{\theta}[\rho_{f}](\mathbf{r}) \right] \phi_{p}(\mathbf{r})$$

$$= \varepsilon_{p} \phi_{p}(\mathbf{r}), \tag{6}$$

which can be considered as a finite-temperature Kohn–Sham (KS) equation with an extra potential term v_{θ} (from the functional derivative of E_{θ}) and ensemble density expression of Eq. (1).

With a similar formulation to KS-DFT, TAO-DFT method can be implemented with SCF machinery, which allows a similarly low computational cost as a conventional KS-DFT calculation. Excited-state extension can be derived through incorporating TAO-SCF into linear-response time-dependent (TD) DFT framework. Within the SCF implementation, the capability of TAO-DFT to capture the static correlation energy has been demonstrated in various systems, including dissociated diatomic molecules, polyacenes, and several carbon-based nonostructures. A4,35,37,38 With these numerical examinations, TAO-DFT appears to be a promising and efficient solution for static correlation.

Despite those successes, there are still two challenging issues. First, a systematic approach to determine the parameter θ is needed, which has been attempted previously, ³⁹ but it is still not perfect as the dissociation potential for H_2 with this approach is still incorrect. Second, the low-lying spurious single excitations were observed in the time-dependent TAO-DFT, ³⁶ similar to those reported with time-dependent density matrix functional theory (TD-DMFT). ^{40,41} This is a direct consequence of fractional occupation numbers, and it limits the capability of directly generalization of many useful directions for TAODFT.

In the present work, we reformulated TAO-DFT into the ground state KS-DFT framework and constructed two new static correlation correction schemes, named revised TAO (rTAO) and rTAO-1, and implemented these methods in post-SCF calculations. In contrast to the original TAO-DFT, which depends on the ensemble density matrix, the reformulated TAO-DFT can be viewed as a regular Kohn–Sham density functional with an orbital-dependent approximation for the exchange–correlation energy. We also developed an efficient optimization method to quantitatively determine the optimal parameter θ . In addition, the usage of single-determinant KS wavefunction as the basic variable in the current approach opens the possibility of an excited-state extension without spurious excitations as in an ensemble approach.

II. THEORY

A. Recasting TAO-DFT in Kohn-Sham formulation

The original form of TAO energy [Eq. (3)] is a functional of the ensemble density matrix at a given fictitious temperature θ (in the units of energy). This is a major difference from the Kohn–Sham approach. Here, we aim to reformulate the TAO approach into a regular Kohn–Sham formalism at zero physical temperature using a single-determinant wavefunction for the reference system. In this way, the terms giving rise to the static correlation can be taken as an orbital-dependent exchange–correlation energy

functional, with which a novel density functional capable of treating static correlation can be formulated.

For a given θ , external potential and particle number, the ground-state energy of TAO-DFT was originally determined with a minimization process over the noninteracting density matrix $\rho_f(\mathbf{r},\mathbf{r}') \equiv \sum_p f_p \phi_p^*(\mathbf{r}) \phi_p(\mathbf{r}')$, as in a finite-temperature KS calculation. However, the TAO functional is not entirely a functional of the density matrix $\rho_f(\mathbf{r},\mathbf{r}')$ because E_θ depends on two density matrices $\rho_f(\mathbf{r},\mathbf{r}')$: one at temperature θ and one at temperature zero. We take an alternative view of the energy optimization and formulate it in terms of the minimization of an orbital functional under the constraints of orthogonal orbitals

$$E_{\text{TAO}}[v_{\text{ext}}, N, \theta] = \min_{\{\phi_p\}} E_{\text{TAO}}[\{\phi_p\}]. \tag{7}$$

The reformulation can be derived from the following revised occupation number expression:

$$f_p = \left[1 + \exp\left(\frac{\langle \phi_p | \hat{h}^{\text{TAO}}[\rho_f] | \phi_p \rangle - \mu}{\theta} \right) \right]^{-1}, \tag{8}$$

where \hat{h}^{TAO} is the one-electron Hamiltonian as given in Eq. (6) and ρ_f represents ensemble density, which is in the form of Eq. (1). This revised expression shows that fractional occupation numbers and the corresponding entropy functional are functionals of orbitals. Under the self-consistency condition, the expression in Eq. (8) simply reproduces that in Eq. (2), where the occupation numbers and the subsequent entropy are expressed as functions of orbital energies.

With Eq. (8), a useful identity relation for any given orbital set can be obtained as follows:

$$\sum_{p} f_{p} \langle \phi_{p} | \hat{h}^{\text{TAO}}[\rho_{f}] | \phi_{p} \rangle = \theta \sum_{p} f_{p} \ln \left[\frac{1 - f_{p}}{f_{p}} \right] + N\mu, \quad (9)$$

with N being the total number of electrons. By employing Eq. (9) in Eq. (3), the total energy of TAO-DFT can be reformulated into an orbital functional as

$$E_{\text{TAO}}[\{\phi_p\}] = -\frac{1}{2} \sum_{p} f_p \langle \phi_p | \nabla^2 | \phi_p \rangle + E_{\text{ext}}[\rho_f] + E_{\text{H}}[\rho_f] + E_{\text{xc}}^{\text{DFA}}[\rho_f]$$
$$+ E_{\theta}[\rho_f] + \theta \sum_{p} f_p \ln f_p + \theta \sum_{p} (1 - f_p) \ln(1 - f_p)$$
(10)

$$= -\frac{1}{2} \sum_{i \in \text{occ.}} \langle \phi_i | \nabla^2 | \phi_i \rangle + E_{\text{ext}}[\rho_f] + E_{\text{H}}[\rho_f] + E_{\text{xc}}^{\text{DFA}}[\rho_f]$$

$$+ E_{\theta}[\rho_f] + \theta \sum_{i \in \text{occ.}} \ln f_i + \theta \sum_{a \in \text{vir.}} \ln(1 - f_a)$$

$$- \int d\mathbf{r} \, v_{\text{eff}}[\rho_f](\mathbf{r}) [\rho_f(\mathbf{r}) - \rho(\mathbf{r})], \qquad (11)$$

in which ρ denotes the KS density, $\rho = \sum_{i \in ooc} \phi_i^* \phi_i$, and v_{eff} is the TAO effective potential employed in Eq. (6). Specifically,

$$v_{\text{eff}}^{\text{TAO}}[\rho_f] = v_{\text{ext}}(\mathbf{r}) + v_{\text{H}}[\rho_f](\mathbf{r}) + v_{\text{xc}}^{\text{DFA}}[\rho_f](\mathbf{r}) + v_{\theta}[\rho_f](\mathbf{r}). \quad (12)$$

Here, a modified entropy-like functional, $\theta \sum_{i \in occ.} \ln f_i + \theta \sum_{a \in vir.} \ln(1-f_a)$, is obtained from the combination of original TAO entropy functional, $\theta \sum_p f_p \ln f_p + \theta \sum_p (1-f_p) \ln(1-f_p)$, and the difference between two orbital energy sums $\sum_p f_p \langle \phi_p | \hat{h}^{\mathrm{TAO}} | \phi_p \rangle - \sum_{i \in occ.} \langle \phi_i | \hat{h}^{\mathrm{TAO}} | \phi_i \rangle$. We note that both the TAO entropy and this new entropy functional inherits the orbital functional nature from the reformulated occupation numbers $\{f_p\}$, which are well-defined for arbitrary input orbitals. Further details in the derivation of Eq. (11) is included in the supplementary material accompanying this work. One can further recast the energy of TAO into a KS energy expression with a TAO-based exchange–correlation energy functional $E_{\mathrm{xc}}^{\mathrm{TAO}}$,

$$E_{\text{TAO}}[\{\phi_{P}\}] = -\frac{1}{2} \sum_{i \in \text{occ}} \langle \phi_{i} | \nabla^{2} | \phi_{i} \rangle + E_{\text{ext}}[\rho] + E_{\text{H}}[\rho] + E_{\text{xc}}^{\text{TAO}}[\{\phi_{P}\}].$$

$$(13)$$

Here, $E_{\rm xc}^{\rm TAO}[\{\phi_p\}]$ represents the modified exchange–correlation functional in the reformulated TAO method,

$$\begin{split} E_{\text{xc}}^{\text{TAO}}[\{\phi_{p}\}] &\equiv E_{\text{xc}}^{\text{DFA}}[\rho_{f}] + \theta \sum_{i \in \text{occ.}} \ln f_{i} + \theta \sum_{a \in \text{vir.}} \ln(1 - f_{a}) \\ &- E_{\text{H}}[\rho] + E_{\text{H}}[\rho_{f}] - \int d\mathbf{r} \, v_{\text{Hxc}}[\rho_{f}](\mathbf{r})[\rho_{f}(\mathbf{r}) - \rho(\mathbf{r})] \\ &+ E_{\theta}[\rho_{f}] - \int d\mathbf{r} \, v_{\theta}[\rho_{f}](\mathbf{r})[\rho_{f}(\mathbf{r}) - \rho(\mathbf{r})]. \end{split} \tag{14}$$

This $E_{\rm XC}^{\rm TAO}$ functional is defined entirely based on rearranging the terms in the original TAO-DFT. However, this reformulation of Eq. (13) offers a new perspective: it is the static correlation missing in the regular DFA that we want to include in XC-functional. This can be expressed as follows:

$$E_{\rm xc}^{\rm TAO}[\{\phi_p\}] = E_{\rm xc}^{\rm DFA}[\rho] + \Delta E_{\rm static}^{\rm TAO}[\{\phi_p\}]. \tag{15}$$

With this TAO exchange-correlation functional reformulated, new and simpler functionals that share similar performance with TAODFT can be developed, which is outlined in Sec. II B.

B. Revised TAO energy functionals

From Eq. (10) of TAO-DFT, one can observe that the entropy term $\theta \sum_p f_p \ln f_p + \theta \sum_p (1 - f_p) \ln (1 - f_p)$ is the crucial component that provides the static correlation, ΔE_{static} , by lowing the overestimated energy when the frontier orbitals become nearly degenerate. However, this entropy term tends to overcorrect and underestimate energy of systems with medium HOMO–LUMO gap, e.g., H_2 with bond length around 1.5 to 3.5 Å.

To compensate the overcorrection of TAO entropy and treat static correlation accurately, we construct two modified total energy functionals. The first one can be considered as a revision of the TAO-DFT functional in Eq. (11),

$$E_{\text{rTAO}}[\{\phi_{p}\}] = -\frac{1}{2} \sum_{p} f_{p} \langle \phi_{p} | \nabla^{2} | \phi_{p} \rangle + E_{\text{ext}}[\rho_{f}] + E_{\text{H}}[\rho_{f}] + E_{\text{xc}}^{\text{DFA}}[\rho_{f}]$$

$$+ \theta \sum_{p} f_{p} \ln f_{p} + \theta \sum_{p} (1 - f_{p}) \ln(1 - f_{p}) \qquad (16)$$

$$= -\frac{1}{2} \sum_{i \in \text{occ.}} \langle \phi_{i} | \nabla^{2} | \phi_{i} \rangle + E_{\text{ext}}[\rho_{f}] + E_{\text{H}}[\rho_{f}] + E_{\text{xc}}^{\text{DFA}}[\rho_{f}]$$

$$+ \theta \sum_{i \in \text{occ.}} \ln f_{i} + \theta \sum_{a \in \text{vir.}} \ln(1 - f_{a})$$

$$- \int d\mathbf{r} \, v_{\text{eff}}[\rho_{f}](\mathbf{r}) [\rho_{f}(\mathbf{r}) - \rho(\mathbf{r})]. \qquad (17)$$

Note that the fractional orbital occupation number f_p is now a functional of the DFA one-electron Hamiltonian \hat{h}_{DFA} , $f_p = f(\langle \phi_a | \hat{h}_{DFA} [\rho_f] | \phi_a \rangle; \theta, \mu)$. The explicit functional forms of \hat{h}_{DFA} and E_{xc}^{DFA} follow the Hamiltonian chosen in the SCF calculation, and the corresponding effective potential functional

$$v_{\text{eff}}[\rho_f] = v_{\text{ext}}(\mathbf{r}) + v_{\text{H}}[\rho_f](\mathbf{r}) + v_{\text{xc}}^{\text{DFA}}[\rho_f](\mathbf{r}). \tag{18}$$

We can see that the static correlation, missing in common DFA, is now captured as

$$\Delta E_{\text{static}}[\{\phi_{p}\}] = E_{\text{ext}}[\rho_{f}] + E_{\text{H}}^{\text{DFA}}[\rho_{f}] + E_{\text{xc}}^{\text{DFA}}[\rho_{f}]$$

$$- E_{\text{ext}}[\rho] - E_{\text{H}}^{\text{DFA}}[\rho] - E_{\text{xc}}^{\text{DFA}}[\rho]$$

$$+ \theta \sum_{i \in \text{occ.}} \ln f_{i} + \theta \sum_{a \in \text{vir.}} \ln(1 - f_{a})$$

$$- \int d\mathbf{r} \, v_{\text{eff}}[\rho_{f}](\mathbf{r}) [\rho_{f}(\mathbf{r}) - \rho(\mathbf{r})], \qquad (19)$$

which can be used in regular KS-DFT calculations in addition to the common functionals.

In contrast to the original TAO-DFT where a modified exchange-correlation functional $E_{\rm xc}^{\rm DFA}$ + E_{θ} is used, here we propose to use only a regular DFA for the exchange-correlation functional $E_{\rm xc}^{\rm DFA}$ with the additional static correlation correction. We do not include the term E_{θ} because it is not necessary and the role of E_{θ} in the original TAO-DFT is contradictory. If we follow the definition in Eq. (4) and do not employ the local density approximation (LDA)³⁴ or gradient expansion approximation (GEA),³⁵ E_{θ} would cancel out the entropy term $\theta \sum_{p} f_{p} \ln f_{p} + \theta \sum_{p} (1 - f_{p}) \ln (1 - f_{p})$ in the total energy [Eq. (10)] and the entropic or the static correlation effect for energetically similar orbitals would be completely missing. Thus, the LDA/GEA approximation in E_{θ} is needed to keep this entropy term in the total energy. Furthermore, it has also been demonstrated in several numerical examples, ^{34,35} especially in those cases with θ values below 50 mHartree, that the contributions of E_{θ} in the LDA/GEA approximation are much smaller than the conventional XC components.

With the new total energy functional, the next step in a standard procedure is to carry out a total energy minimization of $E_{\text{rTAO}}[\{\phi_p\}]$. However, the static correlation functional [Eq. (19)] as well as the total energy functional [Eq. (17)] are not invariant under a unitary rotation of occupied or virtual orbitals, and thus, the conventional SCF framework cannot be applied directly. As an

alternative, we adopt a post-SCF approach using the orbital set from a conventional DFA calculation,

$$E_{\text{rTAO}} = E_{\text{rTAO}} \left[\left\{ \phi_p^{\text{DFA}} \right\} \right]. \tag{20}$$

Moreover, although the effective Hamiltonian in SCF is evaluated with the KS density expression ρ in the revised minimization, all density functionals in rTAO total energy [Eq. (17)], including the occupation numbers $\{f_p\}$ as an implicit functionals of ρ_f via Hamiltonian $\hat{h}_{\mathrm{DFA}}[\rho_f]$, are evaluated with the ensemble density ρ_f as the functionals in Eq. (11). As a consequence, the expression of f_p forms an iterative relation

$$f_p^{[n+1]} = \left[1 + \exp\left(\frac{\langle \phi_p^{\text{DFA}} | \hat{h}_{\text{DFA}} [\{f_q^{[n]}, \phi_q^{\text{DFA}}\}] | \phi_p^{\text{DFA}} \rangle - \mu}{\theta}\right)\right]^{-1}, \tag{21}$$

where [n] denotes the nth iteration. Accordingly,an additional self-consistent treatment is required to determine $\{f_p\}$ and corresponding ensemble density ρ_r .

In order to decompose the iterative expression and reduce the computational complexity, we proposed an alternative approach for evaluating total energy. In this approach, we employ an additional linearization with respect to density difference $\rho_f - \rho$, with Eq. (13). With details provided in the supplementary material, we show that the energy functional becomes

$$E_{\text{rTAO-1}}[\{\phi_{p}\}] = -\frac{1}{2} \sum_{i \in \text{occ.}} \langle \phi_{i} | \nabla^{2} | \phi_{i} \rangle + E_{\text{ext}}[\rho] + E_{\text{H}}[\rho] + E_{\text{xc}}^{\text{DFA}}[\rho]$$

$$+ \theta \sum_{i \in \text{occ.}} \ln f(\langle \phi_{i} | \hat{h}_{\text{DFA}}[\rho] | \phi_{i} \rangle; \theta, \mu)$$

$$+ \theta \sum_{i \in \text{occ.}} \ln [1 - f(\langle \phi_{a} | \hat{h}_{\text{DFA}}[\rho] | \phi_{a} \rangle; \theta, \mu)]. \tag{22}$$

Here, we denote this energy functional with rTAO-1 to separate it from rTAO, the one described by Eq. (17).

The energy expression can be further reduced when a conventional KS-DFA reference is considered, where the first four terms yield the energy of conventional KS-DFA energy

$$E_{\text{rTAO-1}}[\{\phi_{p}\}] = E_{\text{DFA}}[\{\phi_{i}\}] + \Delta E_{\text{static}}^{\text{rTAO-1}}[\{\phi_{p}\}]$$

$$= E_{\text{DFA}}[\{\phi_{i}\}] + \theta \sum_{i \in \text{occ.}} \ln f_{i}[\{\phi_{p}\}]$$

$$+ \theta \sum_{a \in \text{cir}} \ln(1 - f_{a}[\{\phi_{p}\}]).$$
(24)

This total energy can be considered as KS-DFA ground-state energy combined with an entropy-like static correlation correction. A similar entropy-like form of static correlation correction was derived from an adiabatic connection formalism. However, the total energy functional is defined differently in Ref. 42. A comparison to our work [Eq. (22)] with Fig. 4 is also provided in Sec. III B.

Similar to the original TAO-DFT, the orbitals in Eq. (22) are eigenfunctions of a one-electron Hamiltonian $\hat{h}_{\text{DFA}}[\rho]$; therefore, the entropy-like correction (second term) in Eq. (24) can be

evaluated with DFA orbital energies. Thus, the static correlation for arbitrary θ can be obtained without any additional numerical integration once the SCF is converged, which provides a rapid scheme to scan over θ .

III. RESULTS

A. Numerical implementation

We implemented two numerical approaches corresponding to rTAO total energy expressions in Eq. (17) and rTAO-1 in Eq. (22) in a development version of Q-Chem 5.3.⁴³ Both rTAO and rTAO-1 calculations are performed based on results from a conventional DFA SCF calculation or modified SCF that includes $E_{\theta}[\rho]$ in the total energy functional and $v_{\theta}[\rho]$ in the KS equation. An additional self-consistent iteration is attached to the end of SCF to calculate the rTAO occupation numbers and total energy.

All numerical results of TAO-DFT are by default calculated with gradient–expansion approximation (GEA) version of E_{θ} ; for rTAO and rTAO-1, the results calculated without E_{θ} are considered unless specified Fig. 1. The two-electron integrals in SCF calculation are evaluated with the standard quadrature grid EML(50 194),⁴⁴ consisting of 50 Euler–Maclaurin⁴⁵ radial grid points and 194 Lebedev angular grid points per nucleus.

B. Homolytic bond dissociation

The occurrence of static correlation is highly related to nearly degenerate orbitals, which is seen in covalent bond dissociation process, especially in homolytic bond cleavage. Even in the dissociation of H_2 , the simplest molecular system, potential energy curve, is still severely affected by static correlation. In this section, we examine the performances of rTAO and rTAO-1 with bond dissociation reaction.

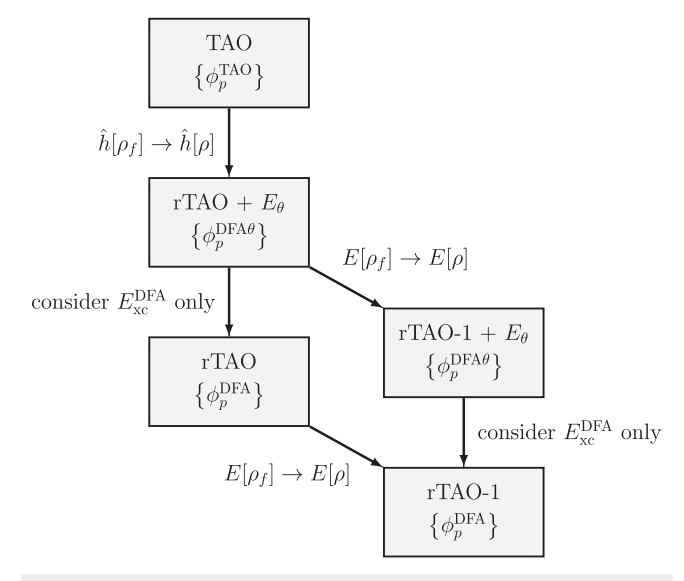


FIG. 1. Schematic illustration for the relationship between TAO-DFT, rTAO, and rTAO-1. Here, $\{\phi_p^{\text{DFA}\theta}\}$ denote the set of eigenfunctions of Hamiltonian $\hat{h}_{\text{DFA}}[\rho] + v_{\theta}[\rho]$.

1. Hydrogen dissociation

Here, we report the potential energy curve for H_2 bond dissociation, a simple σ -bond cleavage. Due to the lack of static correlation, conventional KS-DFT overestimates the energy at the dissociation limit, which, in principle, should be equal to the energy of two isolated hydrogen atoms. It has been shown in the original TAO-DFT that the H_2 can be properly set with θ = 40 mHartree. Figure 2 demonstrates the potential energy curves of TAO-DFT, together with those of rTAO and rTAO-1. For the sake of completeness in comparison, results simulated with rTAO and rTAO-1 combined with E_{θ} are also included.

It is seen that both rTAO and rTAO-1 reproduce the dissociation curves calculated with TAO-DFT in low θ , but rTAOs deviate from TAO-DFT and estimate lower dissociation energies in the high θ cases. This deviation is originated from the increased values of E_{θ} and v_{θ} in TAO-DFT as θ is increased, and, therefore, incorporating rTAOs with E_{θ} and v_{θ} eliminates the difference in high θ regime.

In Fig. 3, we included a detailed comparison of rTAO and rTAO-1 with or without E_{θ} for θ set at 30 or 40 mHartrees, with the latter being suggested as a proper setting for diatomic dissociation in the original TAO-DFT works (Refs. 34 and 35). In Fig. 3, it is seen that that both rTAO-1 and rTAO are able to yield a dissociation profile close to TAO-DFT with a similar θ . In particular, for rTAOs without E_{θ} in Fig. 3(a), the rTAO and rTAO-1 with θ = 30 mHartree yielded potential energy curves that are very close that of coupled-cluster singles and doubles (CCSD). This implies that although rTAOs without the addition of E_{θ} and v_{θ} , which cannot perfectly reproduce the original TAO-DFT, it is still able to precisely describe static correlation with a different θ . In fact, the differences between rTAOs and original TAO due to E_{θ} are negative; thus, the optimal θ for rTAOs evaluated with KS-SCF outputs would be lower than the one for TAO-DFT, in particular, to medium θ regime.

Moreover, we further compare the rTAO-1 to one of the static correlation functionals proposed in Ref. 42, which has a similar expression in entropy-like functional but is defined differently in total energy functional. As shown in Fig. 4, although both methods predict close dissociation limits due to the similar entropy-like correction terms, the functional from Ref. 42 incorrectly described the potential energy in the intermediate region.

2. Ethane C-C bond dissociation

We further tested the C–C bond dissociation in an ethane molecule. Similar to H_2 dissociation, a single σ -bond breaking is considered in the bond dissociation, where the dissociation energy is also overestimated with KS-DFT. The results from rTAO and rTAO-1 are included in Figs. 5(a) and 5(b), in which both rTAO and rTAO-1 does not only reproduce TAO-DFT dissociation curve in low to medium θ without E_{θ} , but also provide a good description in θ = 20 mHartree compared to the multi-reference method, MRCISD + Q.⁴⁶ Accordingly, a θ slightly below 20 mHartree would be suggested for this dissociation curve.

3. Nitrogen molecular dissociation

In the dissociation of N_2 , where a triple bond is broken, it is poorly described even with advanced methods, such as CCSD.

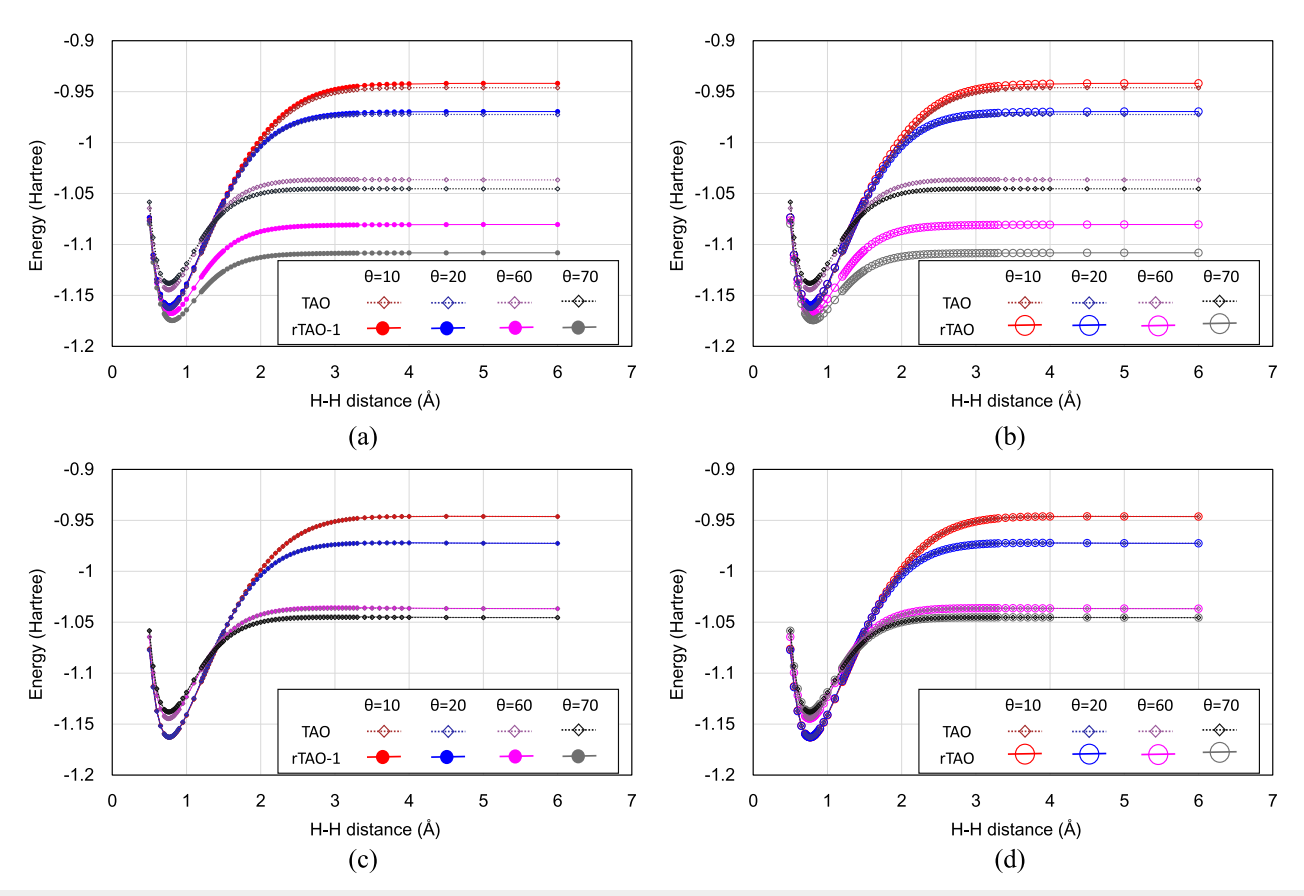


FIG. 2. Comparison between rTAOs and TAO-DFT in ground-state potential energy curves of H_2 molecule with different θ values, calculated with Perdew–Burke–Ernzerhof (PBE) functional and cc-pVDZ basis set. (a) and (b) Potential energy curves for rTAO-1 and rTAO, respectively. (c) and (d) Potential energy curves for modified rTAO-1 and rTAO with extra E_{θ} functionals, respectively.

As shown in Figs. 5(c) and 5(d), the N2 dissociation curves of rTAOs have excellent agreements with TAO-DFT, when θ is set as 30-40 mHartree, similar to the H₂ case. Similar to H₂ and ethane dissociation, it is not necessary to include E_{θ} , with θ set below 40 mHartree. In addition, although rTAO and rTAO-1 results (as well as TAO-DFT) do not match to the MRCISD + Q curves perfectly, they can still improve the overestimated KS dissociation limit and provide a reasonable binding energy. In the case of θ = 30 mHartree, the N-N binding energy is reduced from 16.12 eV in KS-DFT to 9.44 eV with rTAO/rTAO-1 correction, which is proximate to the 8.68 eV binding energy in the multireference configuration interaction with singles and doubles with Davidson correction (MRCISD+Q).⁴⁶ However, with the aim of correcting the dissociation limit, a θ slightly below 30 mHartree would be suggested, which is in a close range of the value determined by the algorithm in Ref. 39.

C. Torsional potential of double bonds

The potential energy for the torsion of a double bond is another standard case for static correlation. In twisting one end of the double bond, the two p-orbital associated with a π -bond are separated

angularly. In the maxima of the torsional energy curves, two *p*-orbitals would be degenerate as a pair of degenerate orbitals. Thus, the torsional potential is one important class of problems for studying the static correlation. Here, torsional potentials in the C–C double bond(s) for ethane and allene (1,2-propadiene) are simulated with both rTAOs.

1. Ethylene

In the torsional potential of ethylene, an overestimated barrier, together with a cusp, is obtained with a commonly used approximation in KS-DFT due to the static correlation problem.

We considered two slightly different reaction paths for the torsional potential in the ethylene molecule. The first one is a pure torsion, in which the C–C bond length is fixed, and the corresponding potential energy curve is shown in Fig. 6(a). The second one is shown in Fig. 6(b) in which the torsion is combined with C–C bond extension, as employed previously. The fundamental difference between these two paths is the HOMO–LUMO gap at the 90° geometry. The HOMO and LUMO obtained from the conventional BYLYP/cc-pVTZ calculation are only nearly degenerate in the pure torsional case with the bond length close to

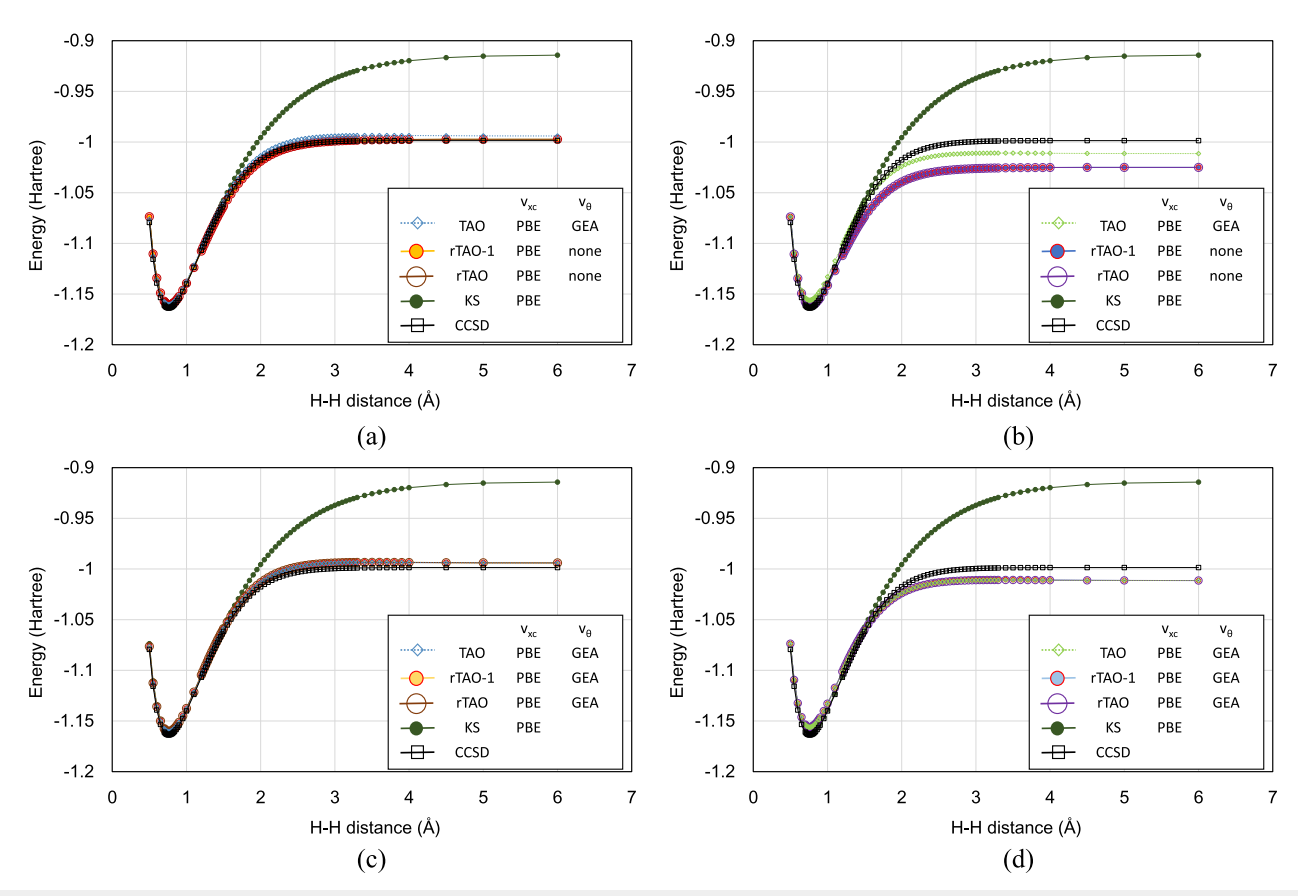


FIG. 3. Ground-state potential energy curves for rTAOs in H_2 bond dissociation: (a) and (b) for rTAOs in $\theta = 30$ and 40 mHartree, respectively; (c) and (d) for rTAOs modified with extra E_{θ} functional in $\theta = 30$ and 40 mHartree, respectively. The results from CCSD, which is numerically exact for the two electron system, conventional KS-DFT and the original TAO-DFT are also included as reference. Calculations were performed with PBE functional for all DFT XC-functionals and cc-pVDZ basis set for all simulations.

the equilibrium geometry, with R_{CC} at 1.339 Å, but the HOMO and LUMO become exact degenerate (with a gap smaller than 10^{-7} eV) when the bond length increased to 1.459 Å. This degenerate feature is also observed in TAO. As a derivative of TAO,

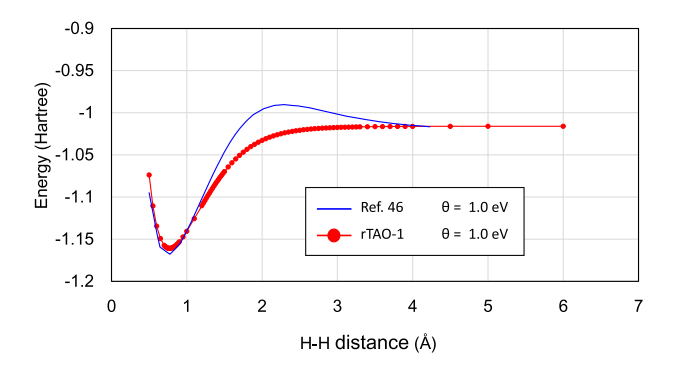


FIG. 4. The blue curve is obtained from "option 1" of Ref. 42, which is calculated with PBE functional, cc-pVTZ basis set, and $\theta = 1$ eV (≈ 36.75 mHartree). The red curve is calculated with rTAO-1 in similar condition, but with a slightly different basis set, cc-pVDZ.

mixing $\langle \phi_{\text{HOMO}} | \hat{h}^{\text{KS}} [\rho_f] | \phi_{\text{HOMO}} \rangle$ and $\langle \phi_{\text{LUMO}} | \hat{h}^{\text{KS}} [\rho_f] | \phi_{\text{LUMO}} \rangle$ is implemented in the rTAO to accelerate the post-SCF iteration of occupation numbers for systems with vanishing KS gap.

As shown in Fig. 6, rTAOs match with the TAO-DFT curves in both trajectories. Furthermore, both rTAOs produce smooth potential energy curves without the incorrect cusp at 90° and reduce the unreasonable barrier height.

According to the original TAO work and the self-consistent θ determination, ^{34,39} the suggested θ value for the fully twisted (with the dihedral angle of HCCH at 90°) ethylene has been 15³⁴ and 15.5 mHartree.³⁹ In Fig. 6(b), the closest curves to the MR-ccCA⁴⁸ result are those calculated with θ = 15 mHartree, which shows a good agreement with previous works.

2. Allene (propadiene)

An allene molecule has two consecutive double bonds linking three C atoms linearly. Here, we simulate the potential for twisting along the two C–C double bonds. Similar to the ethylene case, a conventional DFA calculation predicts a sharp and overestimated transition barrier, but around planner geometry, which deviates from the prediction from complete active space self-consistent field

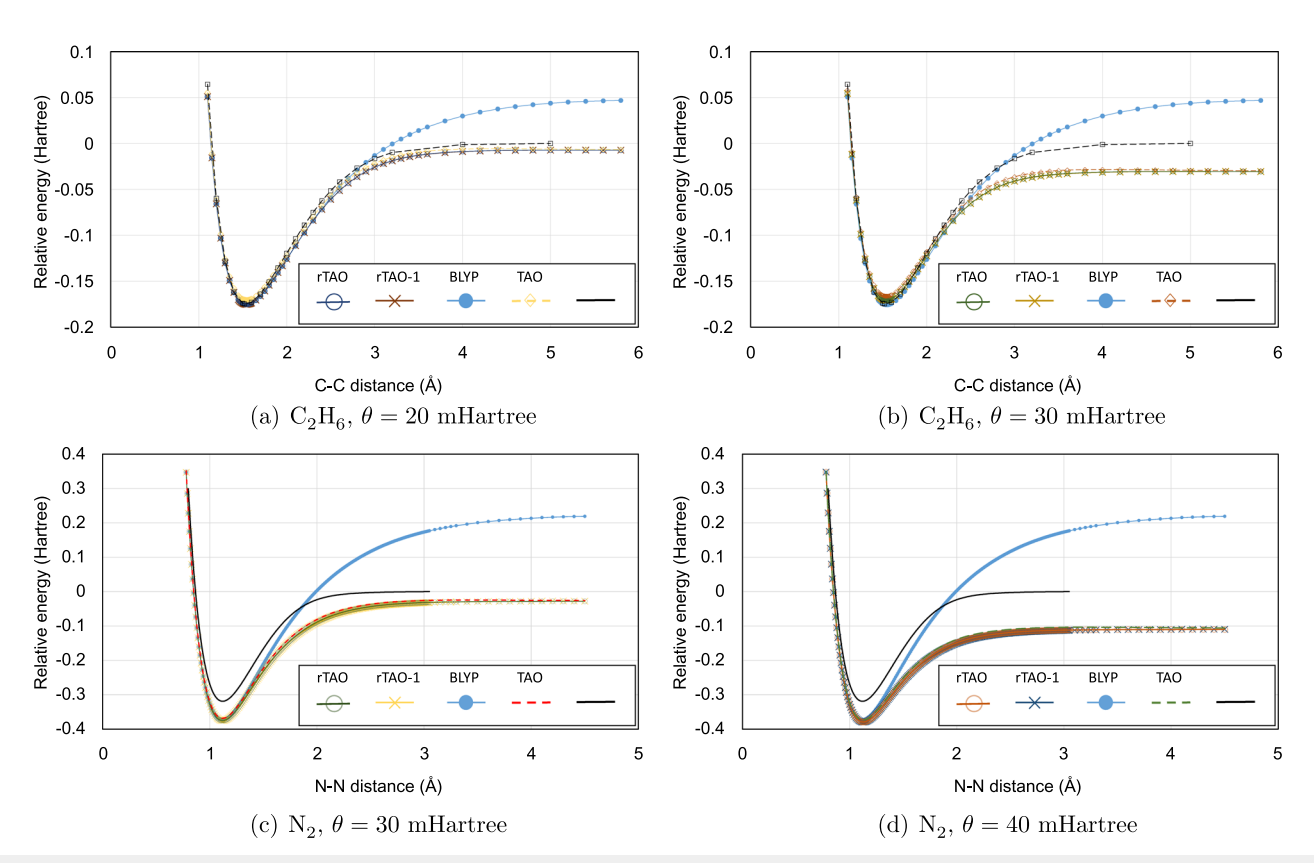


FIG. 5. (a) and (b) Relative potential energy curve of C_2H_6 C–C bond dissociation with different θ values, in which the geometries of CH_3 · fragments are fixed in the dissociation process and the energy of two isolated doublet CH_3 · fragments is set to zero. (c) and (d) Relative potential energy curve of N_2 dissociation with different θ values, where the energy of two isolated quartet N atoms is set to zero. All MRCISD + Q results are obtained from Ref. 46, and so are the structural parameters of ethane and CH_3 · fragment. The BLYP functional and cc-pVDZ basis set are used in all DFT calculations; the quartet N atom and CH_3 · fragment are calculated with conventional unrestricted DFT with the same basis set and functional.

(CASSCF) methods. ^{49,50} In Fig. 7, it is seen that both rTAOs cannot reproduce TAO-DFT energy curves around the edge (0° and 180°) with the same θ . In the case of rTAO-1, the potential curves drops unphysically near maxima, with all θ s tested. Fortunately, although rTAO energies deviates those from those of TAO, it provides a smooth and monotonic curve (between 0° and 90°) and the maximum located at 0° (180°) in the low θ regime, showing a physically correct behavior.

According to the result with low input θ around 0° , we speculate that the deviation of rTAO resulting from TAO is not simply caused by the considerations of E_θ and v_θ as in other molecules. In this particular system, the orbitals and density are strongly affected by whether the fractional occupation numbers are considered in SCF, and as post-SCF methods, the current rTAO and rTAO-1 fail to produce similar density and orbital from the original TAO-DFT, which would be main reason causing the deviation.

D. Application: Determination of θ

We next utilize the post-SCF feature of rTAO-1 to determine the optimal values of θ . In addition to a restricted KS-DFT calculation followed by θ scanning through post-SCF rTAO-1, an auxiliary

calculation as an energy reference is performed simultaneously. Furthermore, to preserve the mild scaling of DFT, the methods with higher computational complexity than KS-DFT are not considered. Here, we chose the unrestricted KS as a suitable candidate due to its reasonable description in energy of the dissociated atoms. Namely, we propose that a proper θ value for the restricted TAO or rTAO should produce energies that are close to those of the unrestricted KS-DFT. Furthermore, we note that this energy match through varying θ can also be considered as an extension of the constancy condition of fractional spins, 26 in which the energy difference between restricted and unrestricted energies of the same density functional approximation is compensated by the static correlation correction.

Two bond-breaking potential energy curves are considered to test the preliminary scheme. First, for the same H_2 dissociation as shown in Figs. 2 and 3, the optimal θ is 30.0 mHartree as determined by matching the energy of the unrestricted PBE (UPBE) calculation at 6 Å, as further demonstrated in Fig. 8(a). While the potential energy curve is the same as presented in Fig. 3(a), we note that the rTAO and rTAO-1 potential curves calculated with this θ value, determined by a UPBE energy value, do not only successfully dissociate H_2 to two isolated H atoms, but they also share the same

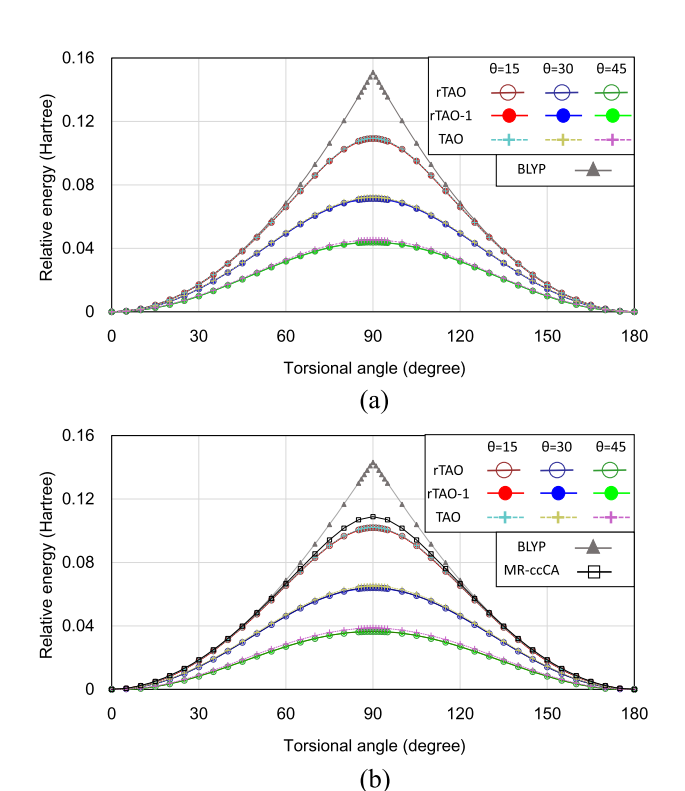


FIG. 6. Comparison between rTAOs and TAO-DFT in the reaction barrier of ethylene (C_2H_4): (a) HCCH torsion at a fixed C–C bond length (1.339 Å) and (b) HCCH torsion with C–C bond length determining by $R_{\rm CC}=1.339+$, 0.12 \sim $L_{\rm HCCH}/90$ Å. $L_{\rm HCCH}/90$ Å. $L_{\rm HCCH}/90$ Å. The results from conventional KS-DFT are included as a reference, and MR-ccCA results from Ref. 48 are presented as a benchmark in (b). The BLYP functional and cc-pVTZ basis set have been used in DFT calculations. Both horizontal axes are HCCH dihedral angles. All energies are relative to zero (or 180°) dihedral angle for HCCH.

dissociation pattern with CCSD, which is equivalent to full CI in a two-electron system.

We have further determined the optimal θ for the torsional potential of ethylene. Following the second path, at 90°, an optimal θ value of 13.9 mHatree is obtained when compared with unrestricted BLYP (UBLYP). As seen in Fig. 8(b), the corresponding barrier is slightly underestimated in comparison to that of MR-ccCA. The θ value can reproduce the MR-ccCA profile around peak at 12.4 mHartree. Both are close but lower than the suggested value in previous studies. ^{34,39}

Moreover, this θ -determination scheme can also be extended to specify a certain θ according to the geometry of the molecule. However, since the static correlation corrections of rTAO and rTAO-1 are insensitive to θ in the geometries where the static correlation is not significant, e.g., H_2 in its equilibrium bond length, and the targeting unrestricted DFA results do not perfectly match the reference methods, especially the intermediate region of bond breaking, using a specific θ for the entire potential energy curve would be sufficient. The preliminary test results of geometry-adapted θ can be found in the supplementary material.

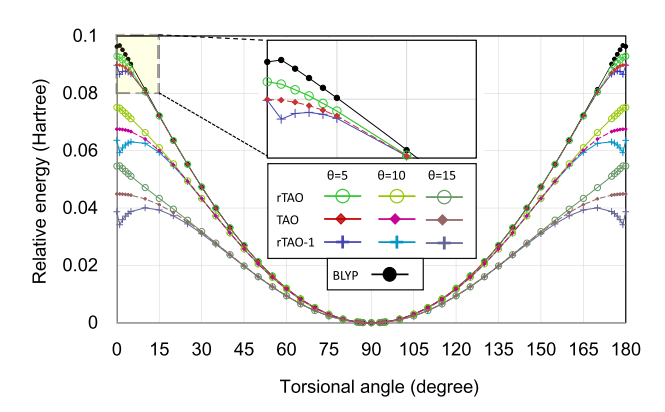
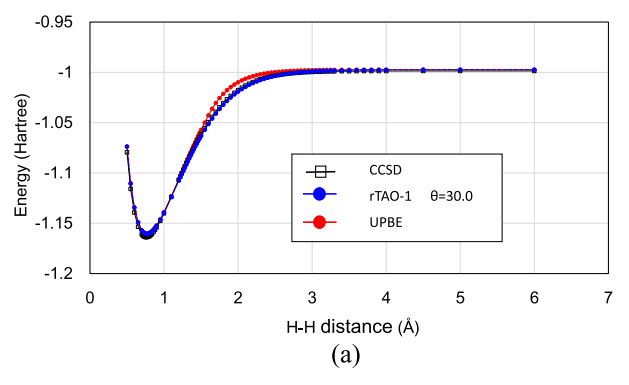


FIG. 7. Comparison between rTAOs, TAO-DFT, and KS-DFT in the torsion of allene (C_3H_4 , 1,2-propadiene). The BLYP functional and cc-pVTZ basis set have been employed in all calculations. The structure parameters are set as $R_{\text{CH}}=1.083$ Å, $R_{\text{CC}}=2.6000$ Å, and $\angle_{\text{HCC}}=121.318^\circ$. All energies of $\angle_{\text{HCCH}}=90^\circ$ are set to zero for each curves. The horizontal axis is HCCH dihedral angle. The energies of 90° dihedral angle for HCCH are set to zero.



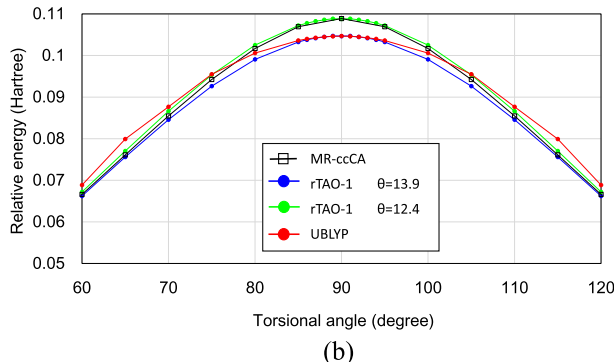


FIG. 8. (a) Potential energy curves of H₂ dissociation, with rTAO-1 calculated with optimal θ that reproduces UPBE energy at H–H distance at 6.0 Å. (b) Torsional potential following the same structural change as in Fig. 6, but rTAO-1 results are calculated with optimal θ that reproduces UBLYP energy at 90°. UBLYP curves are also included in both figures as references.

IV. DISCUSSION

In this work, TAO-DFT is reformulated with a post-SCF correction. Two different approaches, rTAO and rTAO-1, are

derived from the reformulation. Both introduce the static correlation correction to conventional KS-DFT in terms of orbital functionals.

The key step in the reformulation is defining a functional utilizing the single-determinant density ρ instead of ensemble density ρ_f as the working density in the Kohn–Sham scheme, but still keeping the static correlation components from TAO-DFT. As shown in Eqs. (17) and (19), we reformulated TAO as a conventional KS-DFT with an additional correction term for static correlation, which is a functional of both the virtual and occupied orbitals. We also reintroduce the ensemble density ρ_f as an auxiliary quantity to simplify the expression of the static correlation, which is now an orbital-dependent functional.

Similar to the original TAO-DFT, with the additional correction term shown in Eq. (19), there is a lack of unitary rotational invariant property as illustrated in the supplementary material. The one-electron Hamiltonian for all orbitals needed in iterative eigenvalue equations is not available for rTAOs, making it difficult to utilize the conventional SCF scheme. One of the possible alternative approaches is the direct energy minimization through the generalized optimized effective potential approach or orbital optimization. 18,51 However, for the cases of TAO-DFT and rTAOs, there exists non-trivial extra cost corresponded to the orbital rotation step, since the space of orbital transformation required is now the square of number of all the orbitals ($N_{\text{orb.}} \times N_{\text{orb.}}$), which is much larger than that of the previously discussed cases,⁵² which is the number of occupied orbitals times number of virtual orbitals $(N_{\rm occ.} \times N_{\rm vir.})$.

According to the numerical demonstration in various systems, rTAOs can reproduce the potential energy curves of TAO-DFT in low and medium θ regimes, where $\theta \lesssim 40$ mHartree. Although there is an unavoidable deviation from the original TAO with an increase in E_{θ} , which occurs in high θ cases, our study shows that the occurrence of high θ is infrequent in conventional molecular systems. In fact, θ below 40 mHartree is where the original TAO-DFT shows a good agreement with CCSD or multi-reference methods and provides a reasonable description in static correlation, $^{34,35}_{34,35}$ and rTAO and rTAO-1 inherit these advantages. Therefore, rTAOs are not only suitable but also cost-effective options to explore systems with strong static correlation.

In addition, we propose a θ determination scheme accordingly by combining rTAO-1 with the requirement of achieving the same energy between restricted and unrestricted energies under the same density functional approximation. This approach draws a characteristic θ for a particular system without much computational efforts seen in typical scanning approaches. The θ s determined by this scheme are seen to have good agreements with the previous studies in TAO-DFT. With the fact that rTAO and TAO-DFT have similar numerical performance, the θ determined through this scheme can be employed for both the original TAO-DFT and our rTAOs reported in the present work.

V. CONCLUSION

In summary, we reformulated TAO-DFT in KS-DFT framework and developed two treatments to correct single-determinant KS-DFT, rTAO, and rTAO-1 as efficient tools to simulate systems with strong static correlation with post-SCF calculations. Both rTAO and rTAO-1 reproduce the TAO-DFT results in low to medium θ

(\leq 40 mHartree), where the original TAO-DFT can provide a reasonable static correlation correction. In the implementation with inputs purely from conventional DFA calculations, both rTAOs can still provide excellent descriptions in reactions associated with strong static correlation, e.g., diatomic dissociation and torsional rotation on a π -bond, as TAO-DFT, but with different θ . In addition, the post-SCF feature of rTAO-1 also allows a convenient way to explore the system-dependency of θ , which can potentially improve the predictability of both original and revised TAOs. As a direct extension from KS theory, we expect a linear-response-based excited-state implementation without the spurious transition problem as seen in TD-DMFT or TD-TAO-DFT could be developed.

SUPPLEMENTARY MATERIAL

See the supplementary material accompanying this work for details of the theoretical derivation, additional results, and the numeric data for the figures.

ACKNOWLEDGMENTS

C.-P.H. and S.-H.Y. acknowledge support from the Academia Sinica Investigator Award (No. AS-IA-106-M01) and the Ministry of Science and Technology of Taiwan (Grant Nos. MOST 109-2113-M-001-022-MY4, 110-2123-M-001-005, and 109-2926-I-001-502). W.Y. acknowledges support from the National Science Foundation (Grant No. CHE-1900338).

AUTHOR DECLARATIONS

Conflict of Interest

The authors have no conflicts to disclose.

DATA AVAILABILITY

The data that support the findings of this study are available within the article and its supplementary material.

REFERENCES

- ¹P. Hohenberg and W. Kohn, "Inhomogeneous electron gas," Phys. Rev. 136, B864–B871 (1964).
- ²W. Kohn and L. J. Sham, "Self-consistent equations including exchange and correlation effects," Phys. Rev. 140, A1133–A1138 (1965).
- ³R. G. Parr and W. Yang, Density-Functional Theory of Atoms and Molecules (Oxford University Press, Oxford, England, UK, 1989).
- ⁴A. D. Becke, "Perspective: Fifty years of density-functional theory in chemical physics," J. Chem. Phys. **140**, 18A301 (2014).
- ⁵R. O. Jones, "Density functional theory: Its origins, rise to prominence, and future," Rev. Mod. Phys. **87**, 897–923 (2015).
- ⁶N. Mardirossian and M. Head-Gordon, "Thirty years of density functional theory in computational chemistry: An overview and extensive assessment of 200 density functionals," Mol. Phys. 115, 2315–2372 (2017).
- ⁷A. J. Cohen, P. Mori-Sánchez, and W. Yang, "Challenges for density functional theory," Chem. Rev. 112, 289–320 (2012).
- ⁸P. Verma and D. G. Truhlar, "Status and challenges of density functional theory," Trends Chem **2**, 302–318 (2020).
- ⁹I. Y. Zhang and X. Xu, "On the top rung of Jacob's ladder of density functional theory: Toward resolving the dilemma of SIE and NCE," Wiley Interdiscip. Rev.: Comput. Mol. Sci. 11, e1490 (2021).

- ¹⁰ A. D. Becke, "Density functionals for static, dynamical, and strong correlation," J. Chem. Phys. **138**, 074109 (2013).
- ¹¹B. O. Roos, P. R. Taylor, P. E. M. Sigbahn *et al.*, "A complete active space SCF method (CASSCF) using a density matrix formulated super-CI approach," Chem. Phys. **48**, 157–173 (1980).
- ¹²K. Andersson, P. Å. Malmqvist, and B. O. Roos, "Second-order perturbation theory with a complete active space self-consistent field reference function," J. Chem. Phys. **96**, 1218–1226 (1992).
- ¹³P. A. Malmqvist, A. Rendell, and B. O. Roos, "The restricted active space self-consistent-field method, implemented with a split graph unitary group approach," J. Phys. Chem. 94, 5477–5482 (1990).
- ¹⁴D. Casanova and M. Head-Gordon, "Restricted active space spin-flip configuration interaction approach: Theory, implementation and examples," Phys. Chem. Chem. Phys. 11, 9779–9790 (2009).
- ¹⁵G. Li Manni, R. K. Carlson, S. Luo, D. Ma, J. Olsen, D. G. Truhlar, and L. Gagliardi, "Multiconfiguration pair-density functional theory," J. Chem. Theory Comput. 10, 3669–3680 (2014).
- ¹⁶G. Li Manni, R. K. Carlson, S. Luo, D. Ma, J. Olsen, D. G. Truhlar, and L. Gagliardi, "Correction to multiconfiguration pair-density functional theory," J. Chem. Theory Comput. 12, 458 (2016).
- ¹⁷J. Gao, A. Grofe, H. Ren, and P. Bao, "Beyond Kohn-Sham approximation: Hybrid multistate wave function and density functional theory," J. Phys. Chem. Lett. 7, 5143-5149 (2016).
- ¹⁸Z. Chen, D. Zhang, Y. Jin, Y. Yang, N. Q. Su, and W. Yang, "Multireference density functional theory with generalized auxiliary systems for ground and excited states," J. Phys. Chem. Lett. 8, 4479–4485 (2017).
- ¹⁹J. A. Rodríguez-Jiménez, A. Carreras, and D. Casanova, "Short-range DFT energy correction to multiconfigurational wave functions for open-shell systems," J. Chem. Phys. 154, 124116 (2021).
- ²⁰J. Olsen, "The CASSCF method: A perspective and commentary," Int. J. Quantum Chem. 111, 3267–3272 (2011).
- ²¹ A. D. Becke, "Real-space post-Hartree–Fock correlation models," J. Chem. Phys. 122, 064101 (2005).
- ²²E. Proynov, Y. Shao, and J. Kong, "Efficient self-consistent DFT calculation of nondynamic correlation based on the B05 method," Chem. Phys. Lett. 493, 381–385 (2010).
- ²³ E. Proynov, F. Liu, Y. Shao, and J. Kong, "Improved self-consistent and resolution-of-identity approximated Becke'05 density functional model of non-dynamic electron correlation," J. Chem. Phys. 136, 034102 (2012).
- ²⁴ J. Kong and E. Proynov, "Density functional model for nondynamic and strong correlation," J. Chem. Theory Comput. 12, 133–143 (2016).
- ²⁵ N. Q. Su, C. Li, and W. Yang, "Describing strong correlation with fractional-spin correction in density functional theory," Proc. Natl. Acad. Sci. U.S.A. 115, 9678–9683 (2018).
- ²⁶ A. J. Cohen, P. Mori-Sa'nchez, and W. Yang, "Insights into current limitations of density functional theory," Science **321**, 792 (2008).
- ²⁷W. Yang, Y. Zhang, and P. W. Ayers, "Degenerate ground states and a fractional number of electrons in density and reduced density matrix functional theory," Phys. Rev. Lett. **84**, 5172–5175 (2000).
- ²⁸ A. J. Cohen, P. Mori-Sánchez, and W. Yang, "Fractional spins and static correlation error in density functional theory," J. Chem. Phys. 129, 121104 (2008).
 ²⁹Y. Shao, M. Head-Gordon, and A. I. Krylov, "The spin-flip approach within time-dependent density functional theory: Theory and applications to diradicals," J. Chem. Phys. 118, 4807–4818 (2003).
- ³⁰F. Wang and T. Ziegler, "Time-dependent density functional theory based on a noncollinear formulation of the exchange-correlation potential," J. Chem. Phys. **121**, 12191–12196 (2004).
- ³¹Y. A. Bernard, Y. Shao, and A. I. Krylov, "General formulation of spin-flip time-dependent density functional theory using non-collinear kernels: Theory, implementation, and benchmarks," J. Chem. Phys. 136, 204103 (2012).

- ³²Z. Li and W. Liu, "Theoretical and numerical assessments of spin-flip time-dependent density functional theory," J. Chem. Phys. 136, 024107 (2012).
- ³³H. van Aggelen, Y. Yang, and W. Yang, "Exchange-correlation energy from pairing matrix fluctuation and the particle-particle random-phase approximation," Phys. Rev. A 88, 030501 (2013).
- J.-D. Chai, "Density functional theory with fractional orbital occupations,"
 J. Chem. Phys. 136, 154104 (2012).
- 35 J.-D. Chai, "Thermally-assisted-occupation density functional theory with generalized-gradient approximations," J. Chem. Phys. 140, 18A521 (2014).
- ³⁶S.-H. Yeh, A. Manjanath, Y.-C. Cheng, J.-D. Chai, and C.-P. Hsu, "Excitation energies from thermally assisted-occupation density functional theory: Theory and computational implementation," J. Chem. Phys. 153, 084120 (2020).
- ³⁷Q. Deng and J.-D. Chai, "Electronic properties of triangle-shaped graphene nanoflakes from TAO-DFT," ACS Omega 4, 14202–14210 (2019).
- ³⁸S. Seenithurai and J.-D. Chai, "Electronic properties of carbon nanobelts predicted by thermally-assisted-occupation DFT," Nanomaterials **11**, 2224 (2021).
- ³⁹C.-Y. Lin, K. Hui, J.-H. Chung, and J.-D. Chai, "Self-consistent determination of the fictitious temperature in thermally-assisted-occupation density functional theory," RSC Adv. 7, 50496–50507 (2017).
- ⁴⁰ K. J. H. Giesbertz, O. V. Gritsenko, and E. J. Baerends, "The adiabatic approximation in time-dependent density matrix functional theory: Response properties from dynamics of phase-including natural orbitals," J. Chem. Phys. 133, 174119 (2010).
- ⁴¹ K. Pernal, O. Gritsenko, and E. Jan Baerends, "Time-dependent density-matrix-functional theory," Phys. Rev. A **75**, 012506 (2007).
- ⁴²P. Ramos and M. Pavanello, "Static correlation density functional theory," arXiv:1906.06661 [cond-mat.str-el] (2019).
- ⁴³E. Epifanovsky, A. T. B. Gilbert, X. Feng, J. Lee, Y. Mao, N. Mardirossian, P. Pokhilko, A. F. White, M. P. Coons, A. L. Dempwolff *et al.*, "Software for the frontiers of quantum chemistry: An overview of developments in the Q-Chem 5 package," J. Chem. Phys. **155**, 084801 (2021).
- ⁴⁴P. M. W. Gill, B. G. Johnson, and J. A. Pople, "A standard grid for density functional calculations," Chem. Phys. Lett. **209**, 506–512 (1993).
- ⁴⁵C. W. Murray, N. C. Handy, and G. J. Laming, "Quadrature schemes for integrals of density functional theory," Mol. Phys. 78, 997–1014 (1993).
- ⁴⁶C. Li and F. A. Evangelista, "Driven similarity renormalization group: Third-order multireference perturbation theory," J. Chem. Phys. **146**, 124132 (2017).
- ⁴⁷A. Karton, B. Ruscic, and J. M. L. Martin, "Benchmark atomization energy of ethane: Importance of accurate zero-point vibrational energies and diagonal Born-Oppenheimer corrections for a 'simple' organic molecule," J. Mol. Struct. THEOCHEM 811, 345–353 (2007).
- ⁴⁸W. Jiang, C. C. Jeffrey, and A. K. Wilson, "Empirical correction of nondynamical correlation energy for density functionals," J. Phys. Chem. A **116**, 9969–9978 (2012).
- ⁴⁹W. M. Jackson, A. M. Mebel, S. H. Lin, and Y. T. Lee, "Using *ab initio* MO calculations to understand the photodissociation dynamics of CH₂CCH₂ and CH₂C₂," J. Phys. Chem. A **101**, 6638–6646 (1997).
- ⁵⁰M. Gottselig and M. Quack, "Steps towards molecular parity violation in axially chiral molecules. I. Theory for allene and 1,3-difluoroallene," J. Chem. Phys. **123**, 084305 (2005).
- ⁵¹Y. Jin, D. Zhang, Z. Chen, N. Q. Su, and W. Yang, "Generalized optimized effective potential for orbital functionals and self-consistent calculation of random phase approximations," J. Phys. Chem. Lett. 8, 4746–4751 (2017).
- ⁵²Z.-h. Yang, M. R. Pederson, and J. P. Perdew, "Full self-consistency in the Fermi-orbital self-interaction correction," Phys. Rev. A 95, 052505 (2017).
- ⁵³M. R. Pederson, A. Ruzsinszky, and J. P. Perdew, "Communication: Self-interaction correction with unitary invariance in density functional theory," J. Chem. Phys. **140**, 121103 (2014).